COMMUNICATION

Hydrothermal Carbonization of Abundant Renewable Natural Organic Chemicals for High-Performance Supercapacitor Electrodes

Lu Wei, Marta Sevilla, Antonio B. Fuertes, Robert Mokaya, and Gleb Yushin**

Electrical double layer capacitors (EDLCs), often also called supercapacitors, have steadily grown in importance as high-power electrochemical energy storage devices with ultra-long cycle-life[1], sub-second charging,[2] and a very wide operational temperature range,[3] properties that are currently unattainable in Li-ion batteries. The applications of these important devices include use in consumer electronics, uninterruptable power supplies, energy efficient industrial equipment, electric and hybrid electric vehicles and power grid applications.[1]

Energy storage in EDLCs is based on the electrostatic adsorption of electrolyte ions on the large specific surface area of electrically conductive porous electrodes. In spite of the higher capacitance often offered by conductive polymers[4] and metal oxide-based supercapacitors,[5] the greater cycle stability and higher electrical conductivity of porous carbons has led to their use in nearly 100% of commercial devices. Multiple factors affect the performance of carbon-based supercapacitors, the most important being the carbon electrodes' surface chemistry[6] and their pore size distribution (PSD).[7] The ideal pores should be slightly larger than the size of the de-solvated ions. Smaller pores prevent efficient ion electroadsorption,[8] whereas significantly larger pores reduce the capacitance.[7] The negative effect of larger pores may often be noticed during carbon activation studies, when the longer activation time and the resultant larger specific surface area (SSA) commonly leads to capacitance increase only to a surface area of ~1500 $m^2 g^{-1}$ (see previous work[8a,9]). Further increase in activation time significantly increases the average pore size, which results in the saturation or decrease in the carbon specific capacitance.[9] Prior to 2006, the energy storage in carbon-based EDLCs was modeled via the Helmholtz electrical double layer (EDL), which consists of solvated ions adsorbed on the internal carbon pore surface. In 2006, systematic studies by Chmiola et al.[7a] and by Raymundo-Pinero et al.[7b] clearly showed significant enhancement of the specific capacitance in small micropores, where the ion solvation shell becomes highly distorted and partially removed.[7a] The resulting smaller charge separation distance between the ion centers and the pore walls leads to greatly increased capacitance.[7a] In this case ions form a monolayer or a wire inside a carbon pore for slit or cylindrical shaped pores respectively.[10] It is still commonly believed that co-existance of large mesopores with micropores in carbons is required for rapid ion transport and high power characteristics of supercapacitors. Studies on the use of carbon nanotubes (CNTs),[6b,11] carbon onions,[2c,6b] and graphene[2a] with very poor volumetric capacitance but fast rate capabilities were motivated by this hypothesis. However, in our recent studies we demonstrated that ultra-fast ion transport is possible in micropores, provided they have straight shapes with no bottlenecks.[2b] Therefore, microporous carbons with well-controlled PSD and a large surface area of small pores are needed for advanced supercapacitors with improved volumetric and gravimetric energy storage characteristics.

Several methods have been explored for PSD-controlled microporous carbon synthesis for EDLCs. The use of sacrificial zeolite templates for porous carbon synthesis, initially proposed by Kyotani[12] and later adopted by several other groups (see e.g.,[2b,6a,6c]) allow formation of microporous carbons with reproducible properties, high surface area and specific capacitance of 90–150 F g^{-1} in common organic electrolytes.[6a,13] Selective etching of metals from metal carbides and the formation of carbide-derived carbons (CDCs) similarly offer very uniform structure and PSD in sub-nanometer range[14] and specific capacitance of 70–160 F g^{-1} in similar electrolytes,[7a] but commonly suffer from limited SSA of micropores and tortuous pore shape, unless CDC are produced with the help of ordered silica templates.[15]

In spite of these developments, activated carbons (ACs) with a broad PSD and the associated modest specific capacitance (commonly 70–120 F g^{-1} and 30–60 F cm^{-3} in organic electrolytes)[1a,11,16] remain the material of choice for use in commercial supercapacitors, due to well-developed manufacturing technologies, easy production of large quantities, and relatively low production cost. In the view of the authors, the classical porous carbon synthesis route via pyrolysis of organic compounds followed by activation is likely to remain a viable commercial solution. Thus, novel methods for the low-cost synthesis of ACs with larger volumes of straight micropores and better controlled microstructure and PSD are critical for further development and adoption of supercapacitor technology.

L. Wei, Prof. G. Yushin
School of Materials Science and Engineering
Georgia Institute of Technology
Atlanta, GA 30332-0245, USA
E-mail: yushin@gatech.edu
L. Wei
School of Materials Science and Engineering
Northwestern Polytechnical University
Xi'an, Shaanxi 710072, PR China
Dr. M. Sevilla, Prof. A. B. Fuertes
Instituto Nacional del Carbón (CSIC)
P.O. Box 73, Oviedo 33080, Spain
Dr. M. Sevilla, Prof. R. Mokaya
School of Chemistry
University of Nottingham
University Park, Nottingham, NG7 2RD, UK
E-mail: r.mokaya@nottingham.ac.uk

DOI: 10.1002/aenm.201100019

The long-term sustainable energy-efficient economy further demands activated carbon production from naturally grown materials due to their broad availability, low cost and renewable production.

Conventional physical activation of carbonized organics involves partial gas phase oxidation (burning) of carbon by oxygen-containing species such as CO_2 or H_2O to generate pores. This method, however, does not usually create very uniform pore sizes in carbon particles due to faster oxidation of carbon on the particle surface, where the concentration of the gas oxidant is significantly higher. In an attempt to achieve higher surface area and simultaneously eliminate bottle-neck pores while uniformly enlarging the smallest micropores produced in the course of carbonization of organic precursors, Eliad et al. proposed a very interesting route,[8a] in which an equilibrium content of oxygen-containing functional groups are uniformly formed on the porous carbon surface during room temperature treatment in acids. These groups together with the adjusted carbon atoms are later removed via heat treatment at 900 °C. Repetition of the uniform formation of the chemisorbed oxygen functional groups and their removal allows for the uniform pore broadening needed to achieve the optimum PSD.[8a] Unfortunately, the need to use toxic and aggressive substances, an elaborate procedure and multiple high temperature treatments lower the attractiveness of this method for industrial production.

Hydrothermal carbonization is another promising route, offering low-cost, low temperature, environmentally friendly production of novel carbon materials from natural precursors without the need to use toxic chemicals.[17] The process consists of the heat treatment of an aqueous solution/dispersion of organic materials under autogeneous pressure at temperatures as low as 150–350 °C.[17] The resulting solid carbon products (termed hydrochars) generally exhibit uniform chemical and structural properties as well as very high (and tunable) content of oxygen-containing functional groups.[18] Other functionalities (e.g., nitrogen-based) can also be introduced into hydrochars by using dopant-containing carbon precursors or additives.[18a,19] Unfortunately, the hydrochar materials generally possess almost no open porosity[18b,18c] and their heat-treatments at elevated temperatures can only lead to moderate increase in surface area.[20] Until recently,[18d] hydrothermal carbonization was commonly believed to offer limited potential for surface area-sensitive applications.

Here we demonstrate that hydrochars with their networks of uniformly distributed oxygen within the structure may be efficiently transformed into microporous carbons with unusually high specific surface area and pore volume of interconnected micropores. This transformation can be accomplished via simultaneous heat-treatment (and thus uniform removal of the oxygen-containing functional groups from hydrochar carbon surface) and opening of closed and bottle-neck pores by activation. We further show for the first time that the microporous carbons produced from natural precursors via the proposed synthesis route offer outstanding potential for supercapacitor applications and, to our knowledge, exhibit both the highest specific capacitance in one of the most common organic electrolytes and rapid charging/discharging capability.

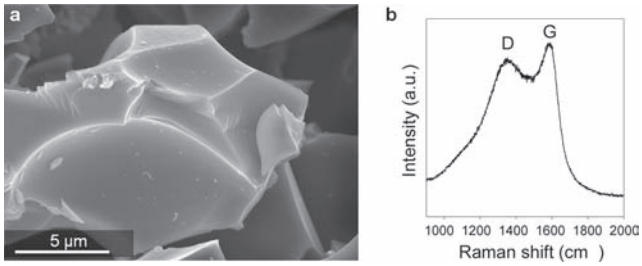

Figure 1. Structure of the microporous carbon materials produced by hydrothermal carbonization: a) a scanning electron microscopy (SEM) image showing typical particle morphology; b) a typical Raman spectra of synthesized carbons.

In our proof-of-concept studies we used several low-cost natural precursors for the formation of microporous carbons: cellulose, potato starch, and eucalyptus wood saw dust. The hydrochars were produced at 230–250 °C, crushed into powders and activated at 700–800 °C. The produced carbons were labelled according to the name of the initial organic precursors and the activation temperature: AC-C700 and AC-C800 (from cellulose), AC-S700 (from starch), AC-W700 and AC-W800 (from wood).

Regardless of the preparation conditions and carbon precursor, the resulting activated carbon particles were 1–20 µm in size and exhibited irregular shape with sharp corners (**Figure 1**a). Raman spectroscopy also revealed little sample-to-sample variations in the shape, position, width and relative integrated intensities of the peaks. Figure 1b shows typical Raman spectra of an activated hydrochar (sample AC-C700). The G-band, located at ~1591 cm^{-1} and corresponding to graphite in-plane vibrations, is slightly upshifted from 1582 cm^{-1},[21] which is common for microporous carbons.[15a,22] The very broad and strong disorder-induced D-band associated with a double-resonance Raman process in disordered carbon[21,23] was located at ~1369 cm^{-1} (Figure 1b). The position and the width of this band may vary, depending on the structure of the disordered carbon, its uniformity and the presence of functional groups.[23]

The nitrogen sorption isotherms of all the synthesized carbon samples (**Figure 2**a) are type-I in the Brunauer classification. Such isotherms exhibit saturation at ~0.3 P/P_0, show no hysteresis between the adsorption and desorption branches and are characteristic for microporous materials. The total specific surface area (SSA) of the synthesized samples estimated using the Brunauer-Emmett-Teller (BET) equation[24] was found to be in the range of 2125–2967 $m^2\ g^{-1}$. These high surface areas are close to the theoretical surface area of graphene (2630 $m^2\ g^{-1}$) and over 5 times higher than that of porous carbons hydrothermally synthesized with the assistance of sacrificial templates reported previously.[25] The pore size distribution, which is particularly important for many pore-size dependant applications, was relatively narrow (Figure 2b) and most of the pore volume and surface area arises from micropores. All carbon samples exhibited virtually no pores >3 nm (Figure 2b). Among the produced and tested carbons, samples AC-C800 and AC-W800, which were activated at the highest temperature (800 °C) showed the largest volume of small mesopores in the range of 2–3 nm. According to non-local density functional theory (NLDFT) calculations, the surface area of the micropores

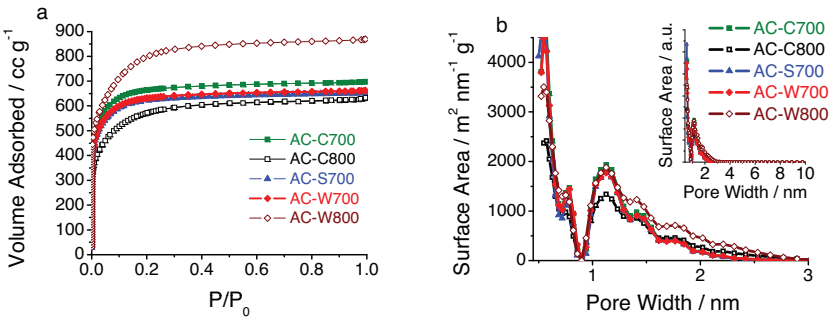

Figure 2. a) N_2 adsorption/desorption isotherms and b) pore size distribution (PSD) for hydrothermally synthesized carbons after activation. The PSD was derived from the N_2 isotherms using non-local density functional theory (NL-DFT). The inset in (b) shows the complete lack of pores >3 nm in these carbons. The dip in the PSD at 0.9 nm is an artifact of the calculations.

in the produced carbons was up to 2387 m^2 g^{-1} (**Table 1**). In contrast to BET-derived total SSA, which may not be very precise for microporous materials due to the strong interaction of adsorbate layers with pore walls and limited space available for multi-layer formation,[26] the DFT calculations are believed to be among the most accurate.[27] The observed micropore DFT-SSA is unusually high. In fact, it exceeds that of most known microporous materials, including zeolites, CDC, conventionally activated carbons and most templated carbons.[2b,6a,14,26,28] Table 1 summarizes the porosity characteristics of our samples.

Electrochemical tests of the hydrothermally synthesized carbon electrodes showed spectacular performance. Cyclic voltammetry (CV) experiments (**Figure 3**) demonstrated a specific capacitance of up to 236 F g^{-1} (100 F cm^{-3}) at a sweep rate of 1 mV s^{-1} (Figure 3b). To the best of our knowledge this is the highest capacitance ever reported for porous carbons in a symmetric two-electrode configuration using tetraethylammonium tetrafluoroborate ($TEABF_4$)/acetonitrile (AN) electrolyte, which is used in most electrochemical capacitors produced in the US. It exceeds the specific capacitance of commercial activated carbons optimized for EDLC applications, such as YP-17D, by 100%. The highest capacitance was demonstrated in the sample produced from wood saw dust. When the scan rate was increased to 10 and then to 100 mV s^{-1} the specific capacitance of this sample decreased to 193 and 173 F g^{-1}, respectively. Such decrease in the specific capacitance is common for activated carbons and likely originates from the insufficient time available for ion diffusion and adsorption inside the smallest pores within large particles. Indeed, at the fastest sweep rate of 100 mV s^{-1} one may clearly observe the distortion of the ideal rectangular shape of the CV, a characteristic of diffusion being the limiting factor for ion adsorption on the EDLC electrode surface.[29] The electrochemical response of our samples (Figure 3a–e) suggests that activation at 800 °C results in a formation of pores having significantly less resistance to the ion motion than the activation at 700 °C (compare shape of the CV curves recorded at 100 mV s^{-1} in Figure 3a,c with the CV curves recorded at 100 mV s^{-1} in Figure 3b,d). The small reduction-oxidation (redox) peaks visible in the CV at ~ 0 and 2 V at the slowest sweep rate are believed to originate from oxygen-containing functional groups remaining in the carbon samples. Such peaks completely disappear at the rate of 10 mV s^{-1}, suggesting relatively slow redox reaction kinetics.[29] The lack of these peaks at 10 mV s^{-1} may further suggest that the pure EDLC capacitance (without pseudocapacitance contribution) in our samples exceeds 193 F g^{-1}.

Figure 3d shows the CV performance of the hydrothermally synthesized carbon sample produced from cellulose and activated at the highest temperature (AC-C800), which demonstrated the lowest capacitance value of 140 F g^{-1}. This value is still noticeably higher than that of conventional activated carbons optimized for EDLC performance. The lower specific surface area of this sample (compare AC-C800 with other samples in Figure 2 and Table 1) clearly led to the smaller ion adsorption capacity. One may notice, however, very good capacity retention at fast sweep rates. Indeed, at a fast sweep rate of 100 mV s^{-1}, the distortion of the rectangular shape of the CV curves in AC-C800 is minimal (Figure 3d). Clearly, the slightly larger volume of small mesopores (2–3 nm pores, Figure 2b) observed in this sample and a possibly smaller number of bottleneck pores may have noticeably improved the ion transport kinetics in this sample.

Figure 3f summarizes changes in the specific capacitance of our samples deduced from the CV measurements recorded at different sweep rates. Data comparison with the performance of YP-17D (which is also produced from a natural precursor) shows doubling the specific capacitance and, thus, doubling the energy density achieved via utilization of the hydrothermal carbonization route. Samples produced from cellulose and starch precursors showed very similar performance (Figure 3f), which may be a result of a similar chemistry of cellulose and starch and the resulting similar size and morphology of porous carbons (Figure 1a), nearly identical pore size distribution (Figure 2b) and microstructure (Figure 1b). This observation

Table 1. Porosity properties of the hydrothermally synthesised materials after activation.

Sample	BET-SSA [m^2 g^{-1}][a)]	Pore Volume [cm^3 g^{-1}][b)]	Micropore SSA [m^2 g^{-1}][c)]	Micropore Volume [cm^3 g^{-1}][c)]
AC-C700	2457	1.08	2080	0.94
AC-C800	2125	0.98	1522	0.74
AC-S700	2273	1.01	2009	0.88
AC-W700	2331	1.03	2002	0.89
AC-W800	2967	1.35	2387	1.20

[a)]BET specific surface area measured for P/P_0 = 0.06-0.14; [b)]Total pore volume measured at P/P_0 = 0.994; [c)]Micropore surface area and volume measured using NL-DFT.

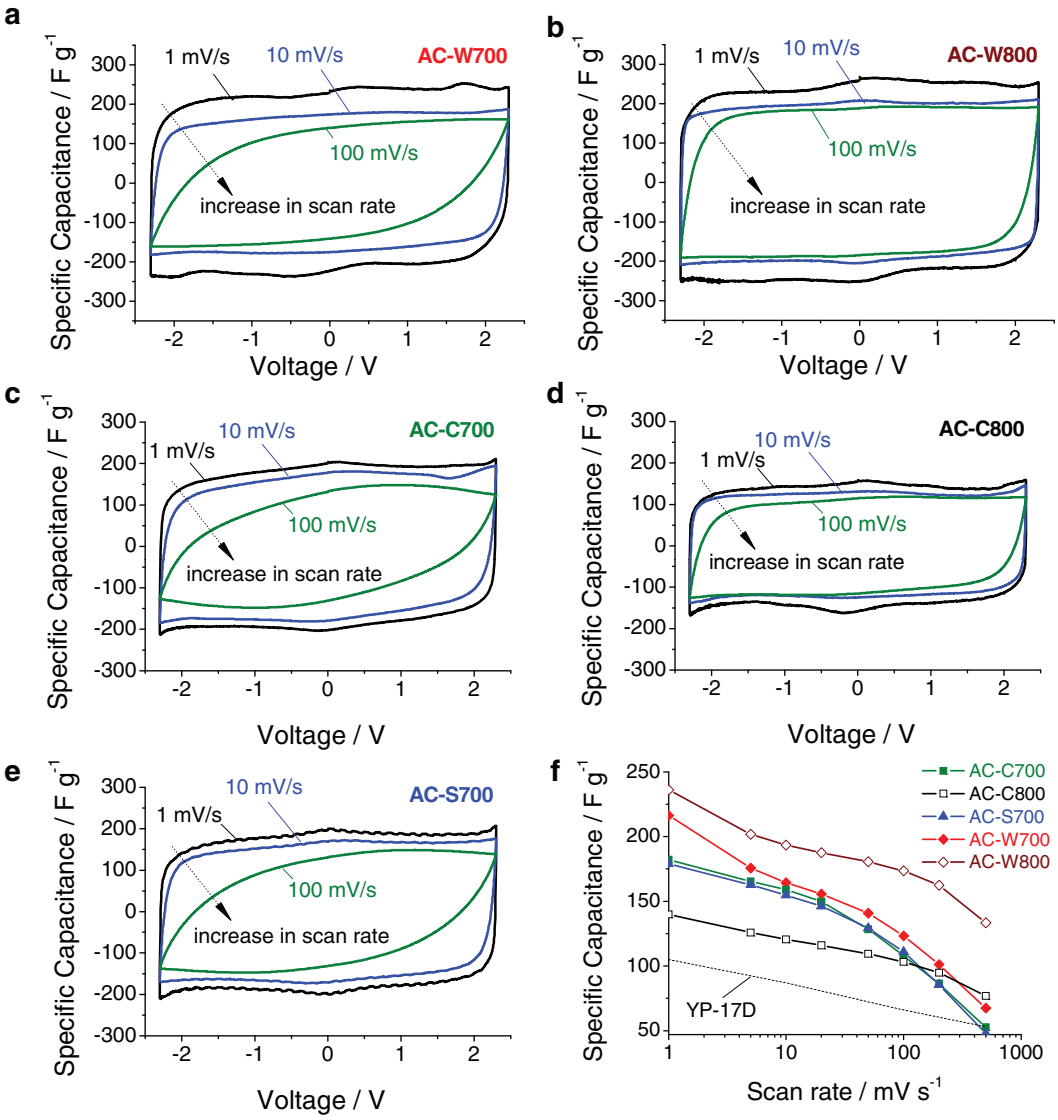

Figure 3. Electrochemical characterization of hydrothermally synthesized carbon materials in 1 M tetraethylammonium tetrafluoroborate ($TEABF_4$) solution in acetonitrile (AN) at room temperature: a–e) cyclic voltammograms (CV) of the carbon samples; f) specific capacitance of carbon samples at different CV scan rates in comparison with that of commercially available YP-17D activated carbon.

also demonstrates the breadth of the natural precursors that can be efficiently used for the formation of activated carbons using the proposed hydrothermal carbonization route.

The performance of supercapacitors in real applications is primarily determined by their charge-discharge (C-D) characteristics, which reveal their energy and power performance. An ideal EDLC with an infinitely fast ion transport should deliver the same energy at virtually any current density. The decrease of capacitance at higher current is generally attributed to increased Ohmic resistance due to the ion "traffic jam" within the particles' micropores or due to the interaction of electrolyte with carbon functional groups or dangling bonds.[6a,6b] Indeed, if only large mesopores were present in carbon, if the diffusion path was minimized to a few nanometers and, finally, if the interactions between the solvent molecules and carbon surface were minimal, the power characteristics of an EDLC electrode and the capacitance retention with increasing current density would increase dramatically.[2a] In our case, however, the electrode thickness is large (~300 μm), the individual particle size is in excess of 1 μm (Figure 1a), the structure has multiple defects (as evident from the very large and broad D-band in the Raman spectra, Figure 1b) and most of the pores are micropores (<2 nm, Figure 2a). Nonetheless, the capacitance retention was very good. The present samples were capable of retaining 64 to 85% of the capacitance when the current density was increased from 0.6 to 20 A g^{-1} (**Figure 4**a). The best capacitance retention was observed in AC-W800 and AC-C800 samples, supporting results of the CV measurements (Figure 3b and Figure 3d). Interestingly, while our carbons were almost entirely microporous, they demonstrated significantly higher capacitance (up to ~175 F g^{-1}) at an ultra-high current density of 20 A g^{-1} than ACs with large mesopores reported to date.[30] This observation confirms our

previous conclusion that the presence of mesopores in carbon electrodes is not required for rapid ion transport, excellent capacity retention and high power characteristics.[2b]

The specific capacitance measured at 0.1 A g^{-1} was found to exhibit a good correlation with the surface area of micropores (Figure 4b). This confirms the previous observations by multiple research groups that larger mesopores offer significantly lower capacitance per unit area.[7]

Electrochemical impedance spectroscopy (EIS) provides complementary information about the frequency response of carbons in EDLCs. The capacitance of the present carbon samples shows saturation at a frequency below ~0.04 Hz, suggesting that nearly equilibrium ion adsorption could be achieved within seconds.

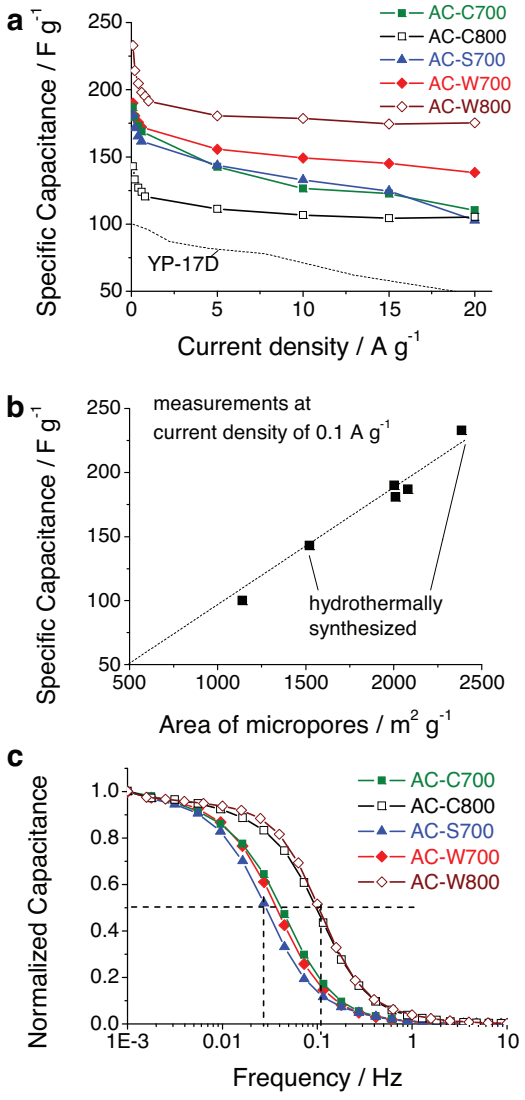

Figure 4. Electrochemical characterization of hydrothermally synthesized carbon materials in 1 M tetraethylammonium tetrafluoroborate ($TEABF_4$) solution in acetonitrile (AN) at room temperature: a) capacitance retention with current density, b) specific capacitance measured at 0.1 A/g as a function of the NL-DFT specific surface area of micropores, c) frequency response. The performance of commercially available YP-17D activated carbon is provided for comparison.

This is similar or slightly faster than what is observed in commercial devices (generally in the range of 10–100 sec). Comparing the frequencies at which capacitance drops to 50% of its maximum value ($f_{0.5}$), we clearly see that the AC-W800 and AC-C800 samples demonstrate the fastest frequency response with $f_{0.5} = 0.1$ Hz. The faster performance of these samples correlates with their slightly larger average pore size (Figure 2b) and better capacitance retention at high sweep rates in the CV measurements (Figure 3f) or higher current densities in C-D tests (Figure 4a).

In summary, we have demonstrated that hydrothermal synthesis may be an attractive route for the transformation of many low-cost naturally grown organic materials into high surface area microporous carbons for supercapacitor applications. Compared to conventionally produced activated carbons used in commercial devices, the proposed route offers ~100% enhancement in the achieved specific capacitance of carbons, which will double the energy density of supercapacitors. Higher carbon activation temperature may lead to lower specific capacitance but better rate performance and faster frequency response of the fabricated devices. Thus, the activation conditions can be tuned for the optimization of the hydrothermally synthesized materials in applications requiring a desired balance of energy and power densities. In contrast to the presently accepted belief, the lack of micropores in the produced materials evidently does not prevent rapid charging of the assembled devices.

Experimental Section

Activated carbon preparation: Hydrochar materials were obtained by hydrothermal carbonization of cellulose (Sigma-Aldrich), potato starch (Sigma-Aldrich), and eucalyptus wood sawdust. An aqueous solution/dispersion (320 g L^{-1}) of the various starting materials was placed in a stainless steel autoclave and heated up to 230 °C (for starch) or 250 °C (for cellulose and wood sawdust) and maintained at the target temperature for 2 h. The resulting solid product (the hydrochar) was recovered by filtration and washed abundantly with distilled water and then dried at 120 °C for 4 h and crushed into powder. To enhance the specific surface area, the hydrochar materials were thoroughly mixed with KOH (Sigma-Aldrich) at a weight ratio of 1:4 = hydrochar/KOH in an agate mortar, heated to 700–800 °C at the heating ramp rate of 3 °C min^{-1} in a horizontal furnace under a nitrogen gas flow and held at this temperature for 1 h. The activated samples were then thoroughly washed several times with 10 wt% HCl to remove inorganic salts, and then with distilled water, until neutral pH was achieved. Finally, the activated carbons were dried in an oven at 120 °C for 3 h. Commercial activated carbon commonly used in commercial supercapacitors (YP-17D, Kuraray Chemicals, Japan) was used for comparison.

Carbon characterization: The Raman spectra were recorded using a Horiva (LabRam HR-800) spectrometer. The source of radiation was a laser operating at a wavelength of 514 nm and a power of 25 mW. The morphologies of the prepared carbon materials were observed via a Leo 1530 (LEO, Osaka, Japan, now Nano Technology Systems Division of Carl Zeiss SMT, USA) scanning electron microscopy (SEM). Nitrogen sorption isotherms of the carbon samples were collected at –196 °C using a Micromeritics ASAP 2020 sorptometer. The surface area was calculated using the BET method based on adsorption data in the relative pressure (P/P_0) range 0.06 to 0.14 and total pore volume was determined from the amount of nitrogen adsorbed at a relative pressure (P/P_0) of 0.99. The pore size distribution (PSD) was determined via a Non Local Density Functional Theory (NLDFT) method using nitrogen adsorption data, and assuming a slit pore model.

Device assembly: Electrodes were prepared by mixing 92 wt% carbon samples and 8 wt% polytetrafluoroethylene (PTFE) in ethanol to form

a slurry. The resulting AC-PTFE composite was then rolled to ~300 μm thick electrodes. The electrode was placed into a vacuum oven (100 °C) overnight to remove moisture and residual hydrocarbons, and then was cut into a circular shape with diameter of 1/2 inch for EDLC electrodes. 2016 stainless-steel coin cells with two symmetrical carbon electrodes separated by two GORE™ PTFE separators (W. L Gore and Associates, USA) of ~25 μm in thickness and ~60% porosity were assembled inside an Ar-filled glove box (<1 ppm of oxygen and H_2O, Innovation Technology, USA). Al foil of 300 μm in thickness roughened using a 600 grit SiC sandpaper and coated by a thin layer (~10 to 20 μm) of carbon coating (BW 525, Superior Graphite) was attached to each electrode and served as current collector. Carbon coating was used to reduce the interfacial resistance between the electrode and the current collector. Purified 1 M tetraethylammonium tetrafluoroborate salt ($TEABF_4$, electrochemical grade, Alfa Aesar) solution in acetonitrile (AN, 99.9%, extra dry, Acros Organics, Geel, Belgium) was used as electrolyte due to its application in most commercial devices.

Electrochemical testing: Cyclic voltammetry (CV) studies were performed using a Solartron 1480A MultiStat (Solartron Analytical, UK) in the voltage range −2.3 V to +2.3 V and in scan rates from 1 to 500 mV s^{-1}. The gravimetric capacitance, C (F g^{-1}), was calculated according to

$$C = \frac{2I}{(dV/dt)m} \quad (1)$$

where I is the current (A), dV/dt is the scan rate (V s^{-1}), and m is the mass (grams) of carbon in each electrode.

Electrochemical impedance spectroscopy (EIS) measurements were carried out using an IM6ex electrochemical workstation (Zahner-Elektrik, Germany) in the frequency range of 1 mHz-100 kHz with a 10 mV AC amplitude. The gravimetric capacitance, C (F g^{-1}), was calculated according to

$$C = \frac{2\cdot|\mathrm{Im}(Z)|}{2\pi f\cdot\left[(\mathrm{Im}(Z))^2+(\mathrm{Re}(Z))^2\right]m} \quad (2)$$

where f is the operating frequency (Hz), Im(Z) and Re(Z) are the imaginary and real parts of the total device resistance (Ohm), and m is the mass (grams) of carbon in each electrode.

Galvanostatic charge-discharge cycle tests (GC) were measured using an Arbin BT-2000 testing system (Arbin Instruments, USA) in the voltage range 0–2.3 V and at charge-discharge current densities between 0.1 and 20 A g^{-1}, based on the mass of a single electrode. The gravimetric capacitance, C (F g^{-1}), was calculated according to

$$C = \frac{2I}{(dV/dt)m} \quad (3)$$

where I is the current (A), dV/dt is the slope of the discharge curve (V s^{-1}), and m is the mass (grams) of carbon in each electrode.

Acknowledgements

This work was partially supported by the AFOSR under grant # FA9550-09-1-0176. M. S. acknowledges the assistance of the Spanish MICINN for the award of a postdoctoral mobility contract.

Received: January 17, 2011
Revised: February 28, 2011
Published online: March 22, 2011

[1] a) P. Simon, Y. Gogotsi, *Nat. Mater.* **2008**, *7*, 845; b) J. R. Miller, P. Simon, *Science* **2008**, *321*, 651.
[2] a) J. R. Miller, R. A. Outlaw, B. C. Holloway, *Science* **2010**, *329*, 1637; b) A. Kajdos, A. Kvit, F. Jones, J. Jagiello, G. Yushin, *J. Am. Chem. Soc.* **2010**, *132*, 3252; c) D. Pech, M. Brunet, H. Durou, P. H. Huang, V. Mochalin, Y. Gogotsi, P. L. Taberna, P. Simon, *Nat. Nanotechnol.* **2010**, *5*, 651.
[3] W. C. West, M. C. Smart, E. J. Brandon, L. D. Whitcanack, G. A. Plett, *J. Eletrochem. Soc.* **2008**, *155*, A716.
[4] I. Kovalenko, D. Bucknall, G. Yushin, *Adv. Funct. Mater.* **2010**, *20*, 3979.
[5] a) J. Li, I. Zhitomirsky, *Colloids Surf., A* **2009**, *348*, 248; b) T. R. Jow, J. P. Zheng, *J. Electrochem. Soc.* **1998**, *145*, 49.
[6] a) C. Portet, Z. Yang, Y. Korenblit, Y. Gogotsi, R. Mokaya, G. Yushin, *J. Electrochem. Soc.* **2009**, *156*, A1; b) C. Portet, G. Yushin, Y. Gogotsi, *Carbon* **2007**, *45*, 2511; c) C. O. Ania, V. Khomenko, E. Raymundo-Pinero, J. B. Parra, F. Beguin, *Adv. Funct. Mater.* **2007**, *17*, 1828; d) D. Hulicova-Jurcakova, M. Seredych, G. Q. Lu, T. J. Bandosz, *Adv. Funct. Mater.* **2009**, *19*, 438; e) D. Hulicova-Jurcakova, M. Kodama, S. Shiraishi, H. Hatori, Z. H. Zhu, G. Q. Lu, *Adv. Funct. Mater.* **2009**, *19*, 1800.
[7] a) J. Chmiola, G. Yushin, Y. Gogotsi, C. Portet, P. Simon, *Science* **2006**, *313*, 1760; b) E. Raymundo-Pinero, K. Kierzek, J. Machnikowski, F. Beguin, *Carbon* **2006**, *44*, 2498.
[8] a) L. Eliad, E. Pollak, N. Levy, G. Salitra, A. Soffer, D. Aurbach, *Appl. Phys. A: Mater. Sci. & Process.* **2006**, *82*, 607; b) G. Salitra, A. Soffer, L. Eliad, Y. Cohen, D. Aurbach, *J. Electrochem. Soc.* **2000**, *147*, 2486.
[9] O. Barbieri, M. Hahn, A. Herzog, R. Kotz, *Carbon* **2005**, *43*, 1303.
[10] a) J. S. Huang, B. G. Sumpter, V. Meunier, *Angew. Chem., Int. Ed.* **2008**, *47*, 520; b) J. S. Huang, B. G. Sumpter, V. Meunier, *Chem.-Eur. J.* **2008**, *14*, 6614.
[11] E. Frackowiak, F. Beguin, *Carbon* **2001**, *39*, 937.
[12] T. Kyotani, Z. X. Ma, A. Tomita, *Carbon* **2003**, *41*, 1451.
[13] H. Nishihara, H. Itoi, T. Kogure, P. X. Hou, H. Touhara, F. Okino, T. Kyotani, *Chem.- Eur. J.* **2009**, *15*, 5355.
[14] G. Yushin, R. K. Dash, Y. Gogotsi, J. Jagiello, J. E. Fischer, *Adv. Funct. Mater.* **2006**, *16*, 2288.
[15] a) Y. Korenblit, M. Rose, E. Kockrick, L. Borchardt, A. Kvit, S. Kaskel, G. Yushin, *Acs Nano* **2010**, *4*, 1337; b) M. Rose, Y. Korenblit, E. Kockrick, L. Borchardt, M. Oschatz, S. Kaskel, G. Yushin, *Small* **2011**, DOI 10.1002/smll.201001898.
[16] a) P. L. Taberna, P. Simon, J. F. Fauvarque, *J. Electrochem. Soc.* **2003**, *150*, A292; b) J. Gamby, P. L. Taberna, P. Simon, J. F. Fauvarque, M. Chesneau, *J. Power Sources* **2001**, *101*, 109.
[17] B. Hu, K. Wang, L. H. Wu, S. H. Yu, M. Antonietti, M. M. Titirici, *Adv. Mater.* **2010**, *22*, 813.
[18] a) M. M. Titirici, M. Antonietti, *Chem. Soc. Rev.* **2010**, *39*, 103; b) M. Sevilla, A. B. Fuertes, *Chem.- Eur. J.* **2009**, *15*, 4195; c) M. Sevilla, A. B. Fuertes, *Carbon* **2009**, *47*, 2281; d) M. Sevilla, A. B. Fuertes, R. Mokaya, *Energy Environ. Sci.* **2011**, DOI: 10.1039/C0EE00347F
[19] R. J. White, M. Antonietti, M. M. Titirici, *J. Mater. Chem.* **2009**, *19*, 8645.
[20] P. Kim, J. B. Joo, W. Kim, J. Kim, I. K. Song, J. Yi, *Catal. Lett.* **2006**, *112*, 213.
[21] a) F. Tuinstra, J. L. Koenig, *J. Chem. Phys.* **1970**, *53*, 1126; b) R. J. Nemanich, S. A. Solin, *Phys. Rev. B* **1979**, *20*, 392.
[22] G. Yushin, E. Hoffman, A. Nikitin, H. Ye, M. W. Barsoum, Y. Gogotsi, *Carbon* **2005** *44*, 2075.
[23] A. C. Ferrari, J. Robertson, *Philos. Trans. Roy. Soc. -Math. Phys. Eng. Sci.* **2004**, *362*, 2477.
[24] S. Brunauer, P. Emmett, E. Teller, *J. Am. Chem. Soc.* **1938**, *60*, 309.
[25] M. M. Titirici, A. Thomas, M. Antonietti, *Adv. Funct. Mater.* **2007**, *17*, 1010.
[26] R. T. Yang, *Adsorbents: Fundamentals and Applications*, John Wiley & Sons, Inc., Hoboken, NJ **2003**.
[27] J. Jagiello, M. Thommes, *Carbon* **2004**, *42*, 1227.
[28] C. Portet, G. Yushin, Y. Gogotsi, *J. Electrochem. Soc.* **2008**, *155*, A531.
[29] B. E. Conway, *Electrochemical Supercapacitors*, Vol. *1*, Kluwer Academic/Plenum Publishers, New York, USA **1999**.
[30] D. W. Wang, F. Li, M. Liu, G. Q. Lu, H. M. Cheng, *Angew. Chem., Int. Ed.* **2008**, *47*, 373.